Early redox, Src family kinase, and calcium signaling integrate wound responses and tissue regeneration in zebrafish

Sa Kan Yoo,[1] Christina M. Freisinger,[2,3] Danny C. LeBert,[4] and Anna Huttenlocher[2,3]

[1]Program in Cellular and Molecular Biology, [2]Department of Pediatrics, [3]Department of Medical Microbiology and Immunology, and [4]Cellular and Molecular Pathology Graduate Program, University of Wisconsin-Madison, Madison, WI 53706

Tissue injury can lead to scar formation or tissue regeneration. How regenerative animals sense initial tissue injury and transform wound signals into regenerative growth is an unresolved question. Previously, we found that the Src family kinase (SFK) Lyn functions as a redox sensor in leukocytes that detects H_2O_2 at wounds in zebrafish larvae. In this paper, using zebrafish larval tail fins as a model, we find that wounding rapidly activated SFK and calcium signaling in epithelia. The immediate SFK and calcium signaling in epithelia was important for late epimorphic regeneration of amputated fins. Wound-induced activation of SFKs in epithelia was dependent on injury-generated H_2O_2. A SFK member, Fynb, was responsible for fin regeneration. This work provides a new link between early wound responses and late regeneration and suggests that redox, SFK, and calcium signaling are immediate "wound signals" that integrate early wound responses and late epimorphic regeneration.

Introduction

Tissue injury immediately induces a barrage of wound responses. Depending on the tissue, wound size, age, and the organism, wound responses can lead to either scar formation or tissue regeneration. Certain teleosts and amphibians regenerate fins and limbs after surgical resection. How regenerative animals sense initial tissue injury and transform the wound signals into regenerative growth is a fundamental question. Wounds generate reactive oxygen species (ROS), specifically hydrogen peroxide (H_2O_2), in phylogenetically diverse organisms, including plants, *Drosophila melanogaster*, zebrafish, and mammals (Orozco-Cárdenas et al., 2001; Roy et al., 2006; Niethammer et al., 2009; Moreira et al., 2010). H_2O_2 mediates initial recruitment of immune cells to damaged tissues in *Drosophila* and zebrafish (Niethammer et al., 2009; Feng et al., 2010; Moreira et al., 2010; Yoo et al., 2011). ROS, such as H_2O_2, inactivate phosphatases and also directly regulate kinases through oxidation of specific cysteine residues (Giannoni et al., 2005; Bienert et al., 2006; Rhee, 2006; Poole and Nelson, 2008; Paulsen and Carroll, 2010; Yoo et al., 2011). Recently, we found that a Src family kinase (SFK), Lyn, functions as a redox sensor that mediates early neutrophil wound attraction in zebrafish larvae (Yoo et al., 2011). Here, using zebrafish larval tail fins as a model to study wound responses and tissue regeneration, we find that immediate wound-induced redox, SFK, and calcium signaling in epithelia are required for late epimorphic regeneration of amputated fins. A SFK member, Fynb, was responsible for fin regeneration. This work provides new insight into how regenerative animals sense initial tissue injury and how the wound signals are transformed into regenerative growth.

Results and discussion

While studying the function of H_2O_2 and SFKs in neutrophils during wound responses in zebrafish larvae at 3 d postfertilization (dpf), we found that wounding induced SFK activation in epithelial cells. We performed tail transection of 3-dpf larvae and detected autophosphorylation of the activation loop tyrosine of SFKs. SFKs were strongly activated at wounded epithelia within 2 h after wounding, which gradually returned to the basal activity level by 6 h after wounding (Fig. 1 A). The immunostaining

S.K. Yoo and C.M. Freisinger contributed equally to this paper.

Correspondence to Anna Huttenlocher: huttenlocher@wisc.edu

Abbreviations used in this paper: dpf, day postfertilization; DPI, diphenyleneiodonium; Duox, dual oxidase; Erk, extracellular signal–regulated kinase; MO, morpholino; pSFK, phosphorylated SFK; ROS, reactive oxygen species; SFK, Src family kinase.

The Rockefeller University Press $30.00
J. Cell Biol. Vol. 199 No. 2 225–234
www.jcb.org/cgi/doi/10.1083/jcb.201203154

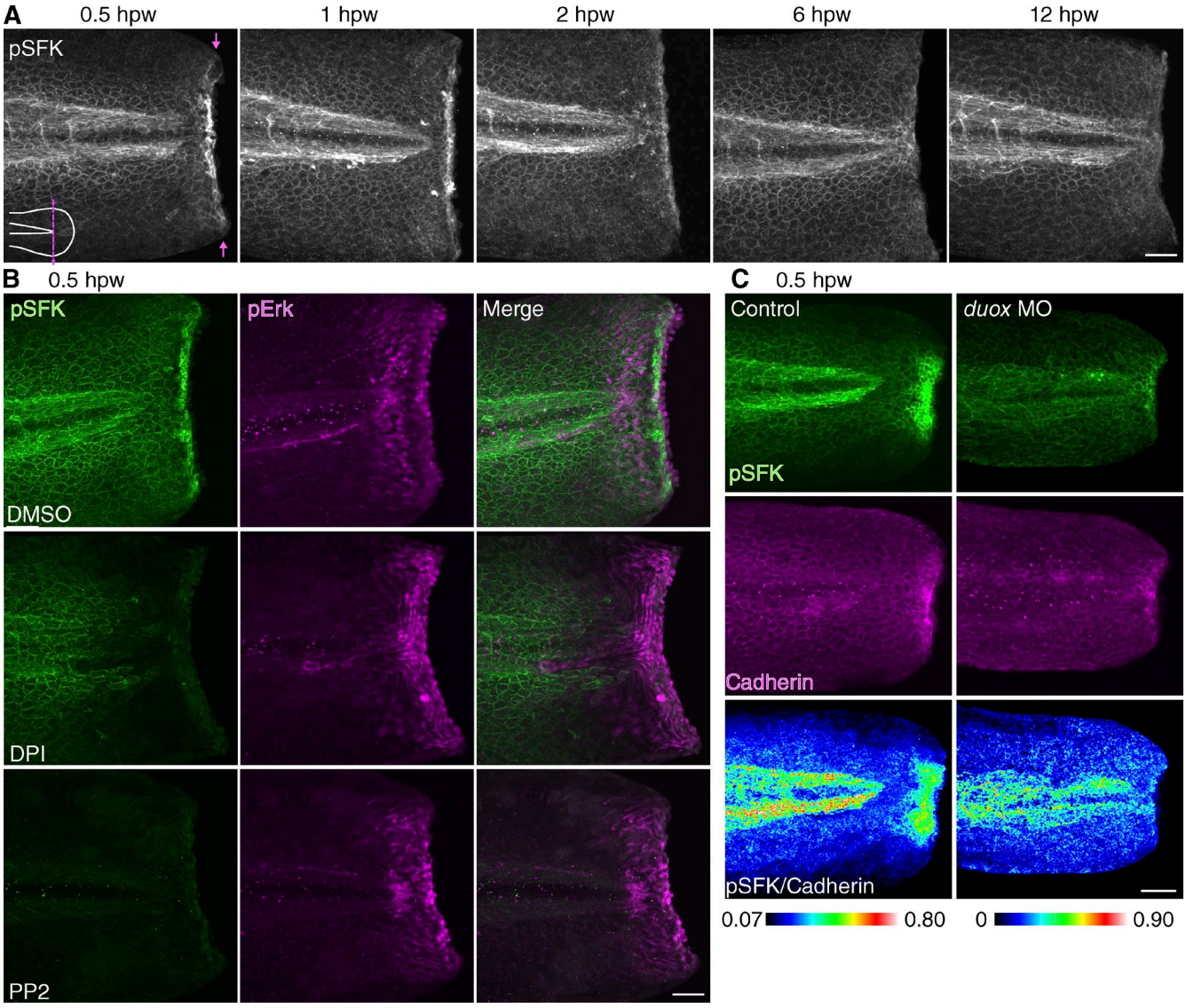

Figure 1. **Redox and SFK signaling at wounds.** (A) Immunofluorescence of pSFK (phosphorylation of SFK activation loop tyrosine) in 3-dpf larvae at various time points. Arrows indicate the position of tail transection. The dotted line is the position of tail transection. (B) Immunofluorescence of pSFK and pErk in 3-dpf larvae at 30 min after tail transection. DPI and PP2 inhibit SFK activation at wounds but not Erk activation. (C) Immunofluorescence of pSFK and Cadherin in 2.5-dpf larvae at 30 min after tail transection. hpw, hour postwounding. Bars, 50 µm.

of phosphorylated SFKs (pSFKs) was not caused by tissue volume increases at wounds because ratiometric analysis demonstrated that more pSFK signals were localized at wounded sites compared with tdTomato (a cytoplasmic fluorescent protein) in epithelial cells or pan-Cadherin staining (Fig. S1, A and B). SFK activation was not detected without wounding or immediately after wounding (Fig. S1, C and D). We also confirmed SFK activation at wounds using a second monoclonal antibody for pSFK (Fig. S1 E).

The mechanism of SFK activation has been extensively investigated over the past several decades (Sicheri et al., 1997; Xu et al., 1997; Martin, 2001; Yeatman, 2004). In an inactive state, SFKs maintain inhibitory intramolecular interactions. Dephosphorylation of the C-terminal phosphotyrosine releases the inhibitory configuration to an open conformation, allowing trans-autophosphorylation of the activation loop tyrosine, thereby fully activating SFKs. In addition to this classical mode of SFK activation, SFKs are also regulated by cysteine oxidation (Giannoni et al., 2005; Kemble and Sun, 2009; Yoo et al., 2011). Thus, we tested whether ROS generated at wounds activate SFKs in epithelia in a similar manner to ROS-mediated activation of Lyn in neutrophils (Yoo et al., 2011). Inhibition of ROS using short transient inhibition of NADPH oxidases with diphenyleneiodonium (DPI) or SFKs with PP2 impaired SFK activation at wounded tissue (Fig. 1 B). In addition, morpholino (MO) antisense oligonucleotide-mediated knockdown of dual oxidase (Duox), which is responsible for H_2O_2 generation at wounds (Niethammer et al., 2009), inhibited SFK activation (Fig. 1 C). We also investigated the effects of ROS and SFK inhibition on extracellular signal–regulated kinase (Erk), which is activated downstream of H_2O_2-Lyn signaling in neutrophils (Yoo et al., 2011). Interestingly, injury

activated Erk around wounds, but Erk activation was independent of ROS or SFK (Fig. 1 B).

A recent study suggested that genetic knockdown of Duox inhibits tail fin regeneration in zebrafish larvae (Rieger and Sagasti, 2011). This prompted us to investigate whether transient inhibition of ROS and SFK at the time of wounding impairs epimorphic regeneration in zebrafish larvae (Fig. 2 A). We found that even short treatment, starting from 1 h before wounding and ending at 1 h after wounding, with DPI or PP2 impaired late regeneration at 3 d after wounding (Fig. 2, B and C). Drug treatment at 3–5 h after wounding did not impact fin regeneration (Fig. S1, F and G). This suggests that the specific signals that occur within 1–2 h of wounding are critical for late regeneration. The pharmacological treatment did not affect fin length without wounding (Fig. S1 G). As a control, PP3, which is structurally related to PP2 but does not inhibit SFKs, did not impair fin regeneration (Fig. S1 H). Zebrafish larval fin regeneration is mediated by cell proliferation in the blastema (Mathew et al., 2007; Ishida et al., 2010; Poss, 2010; Tanaka and Reddien, 2011; Yoshinari and Kawakami, 2011). To evaluate blastemal cell proliferation in regenerating fins, we quantified mitotic cells in tail fins, counting cells positive for phosphorylated histone H3, a marker of mitosis (Nachtrab et al., 2011). Inhibition of ROS and SFKs decreased cell proliferation in wounded fins (Fig. 2, D and E).

Next, we investigated whether inflammation is involved in the regeneration defects induced by drug treatments. When larvae were treated with DPI or PP2 around the time of wounding (1 h before and after wounding), the short treatments inhibited early neutrophil wound attraction at 1 h after wounding (Fig. S2, A and B), as we previously reported (Yoo et al., 2011). However, the treatment increased neutrophil accumulation at wounds at 6 h after wounding, when inflammation is normally resolved. On the other hand, pharmacological treatment with DPI or PP2 starting 1 h after wounding did not affect late neutrophil recruitment to wounds (Fig. S2, A and B). The results suggest that early events that occur within 1 h of wounding are involved in late resolution of inflammation. The early events that regulate late resolution most likely occur outside of neutrophils because neutrophil reverse migration away from wounds is independent of SFKs (Mathias et al., 2006; Yoo and Huttenlocher, 2011; Yoo et al., 2011). Impairment of inflammatory resolution through ROS and SFK inhibition persisted at 3 d after wounding (Fig. 2, F and G). Inflammation inhibits wound healing in mice under certain conditions (Martin, 1997; Martin and Leibovich, 2005), suggesting that inflammation could be upstream of regenerative defects in zebrafish. To investigate this possibility, we depleted myeloid cells using MO-mediated knockdown of Pu.1, a transcription factor required for myeloid cell development (Rhodes et al., 2005). We found that *pu.1* MO did not alter the regeneration defects induced by DPI or PP2 (Fig. 2 H). Efficiency of *pu.1* MO-mediated neutrophil depletion was confirmed by loss of fluorescence in transgenic *Tg(mpx:Dendra2)* (Yoo and Huttenlocher, 2011) and neutrophil staining with Sudan black (Fig. 2, I and J; Le Guyader et al., 2008). Thus, neutrophilic inflammation did not cause the regeneration defect in zebrafish larvae treated with PP2 or DPI. This is consistent with previous findings that inflammation does not have major roles in epimorphic regeneration in zebrafish larvae (Mathew et al., 2007; Rieger and Sagasti, 2011).

Next, we considered whether there are other early wound signals that impact late regeneration. In *Caenorhabditis elegans*, a rapid calcium (Ca^{2+}) wave occurs immediately after injury, and wound-induced Ca^{2+} signaling is important for wound healing (Xu and Chisholm, 2011; Wood, 2012). Thus, we investigated whether injury also induces Ca^{2+} flashes in zebrafish. We expressed the Ca^{2+} sensor GCaMP3 (Tian et al., 2009) in zebrafish larvae. Wounding induced a very rapid and transient Ca^{2+} wave that spreads from the site of injury and persisted for 3–5 min after wounding (Fig. 3, A and B; and Video 1). Depletion of Ca^{2+} in the ER with thapsigargin blocked the wound-induced Ca^{2+} flashes (Fig. 3 C and Video 2), indicating that Ca^{2+} is released from internal stores upon wounding. DPI or PP2 treatment did not block wound-induced Ca^{2+} flashes, and thapsigargin treatment had no effect on the activation of SFK and Erk or the H_2O_2 burst (Fig. S3 A and Fig. 3, D and E), indicating that early wound-induced Ca^{2+} flashes are independent of initial redox and SFK signaling or Erk signaling. However, treatment with thapsigargin or U73211 (an inhibitor for PLC, which liberates calcium from internal stores) at the time of wounding impaired late regeneration (Fig. 3, F and G). Transient inhibition of calcium signaling did not impair development without wounding. We also found that inhibition of wound-induced Erk activation impaired late regeneration (Fig. S3 B), consistent with previously published findings (Ishida et al., 2010). Our data suggest that wounding initiates at least three early signaling events, including H_2O_2-SFK, Ca^{2+}, and Erk signaling, which seem to regulate late regeneration through independent pathways. We focused on how early redox and SFK signaling regulates regeneration.

We considered whether regeneration-defective wounds previously generated with DPI or PP2 treatment have truly lost their regenerative capacity. We investigated whether secondary wounds could induce regeneration in fins that had been previously wounded in the presence of DPI or PP2 treatment. To test this, we wounded zebrafish in the presence of DPI or PP2 at 2 dpf and then rewounded larvae the next day in the absence of drugs (Fig. 4 A). Interestingly, secondary wounds induced complete regeneration in what would normally be regeneration-defective fins (Fig. 4, B and C). The second injury induced SFK activation at wounds similar to the first wound regardless of conditions at the first wound (Fig. 4 D). This indicates that regeneration-defective wounds still maintain a regenerative capacity, which can be activated with "proper" stimulation under optimal conditions.

To identify specific SFKs that mediate fin regeneration, we purified mRNA from the caudal tip of the larval fin and also sorted GFP-positive epithelial cells from a transgenic line, *tg(krt4-GFP)*, using FACS (Fig. 5 A and B; Gong et al., 2002). Analysis of EST profiles in UniGene (NCBI) suggested that *src*, *yes*, *fyna*, *fynb*, and *yrk* might be expressed in zebrafish fins. RT-PCR detected *yes* and *fynb* in both resected tail fins and sorted epithelial cells (Fig. 5 A). Thus, it is likely that epithelial cells in the tail fin relatively enrich transcripts for *yes* and *fynb*. To investigate whether one or both of these SFKs are important

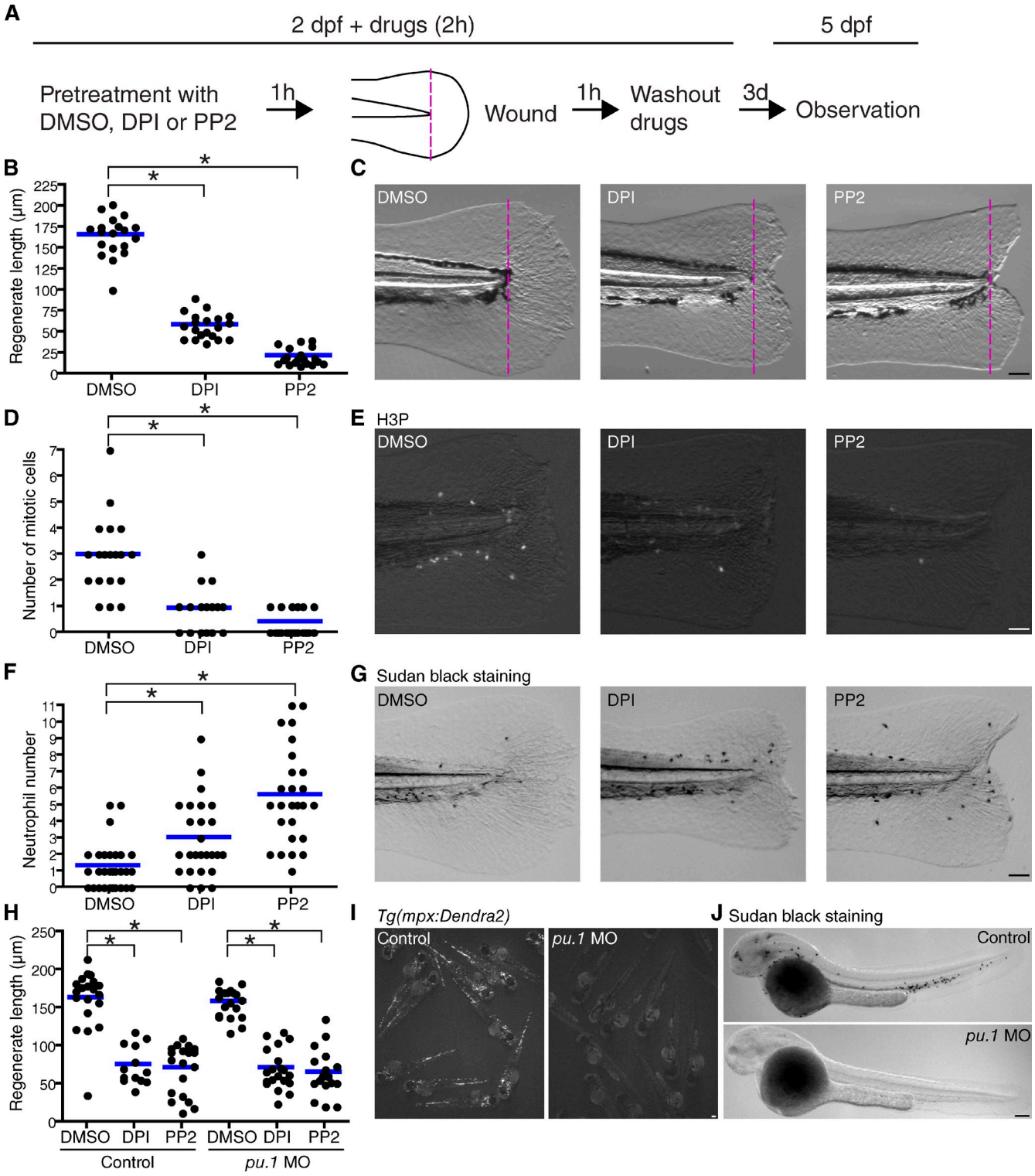

Figure 2. **Early redox and SFK signaling regulates late epimorphic regeneration.** (A) Diagram of regeneration assays using zebrafish larval tail fins. (B) Quantification of regenerated tail fin length at 3 d after wounding (DMSO: 19 larvae; DPI: 20 larvae; PP2: 19 larvae). (C) Representative pictures used for quantification in B. Dotted lines indicate tail transection. (D) Quantification of blastemal proliferation at 36 h after wounding (DMSO: 19 larvae; DPI: 19 larvae; PP2: 21 larvae). Mitotic cells were detected using an antibody for phosphorylated histone H3 (H3P). (E) Representative pictures used for quantification in D. (F) Quantification of neutrophil recruitment to wounded fins at 3 d after wounding (DMSO: 30 larvae; DPI: 25 larvae; PP2: 25 larvae). (G) Representative pictures of Sudan black staining used for quantification in F. (H) Quantification of regenerated tail fin length at 3 d after wounding in control larvae and *pu.1* MO-injected larvae (control/DMSO: 20 larvae; control/DPI: 13 larvae; control/PP2: 19 larvae; *pu.1* MO/DMSO: 20 larvae; *pu.1* MO/DPI: 20 larvae; *pu.1* MO/PP2: 20 larvae). (I) Fluorescent pictures of 2.5-dpf *Tg(mpx:Dendra2)*, which expresses Dendra2 specifically in neutrophils. (J) Sudan black staining of control larvae and *pu.1* MO-injected larvae at 2.5 dpf. *, $P < 0.05$; one-way ANOVA with Dunnett's posttest. Horizontal lines indicate means. Bars: (C, E, and G) 50 µm; (I and J) 100 µm.

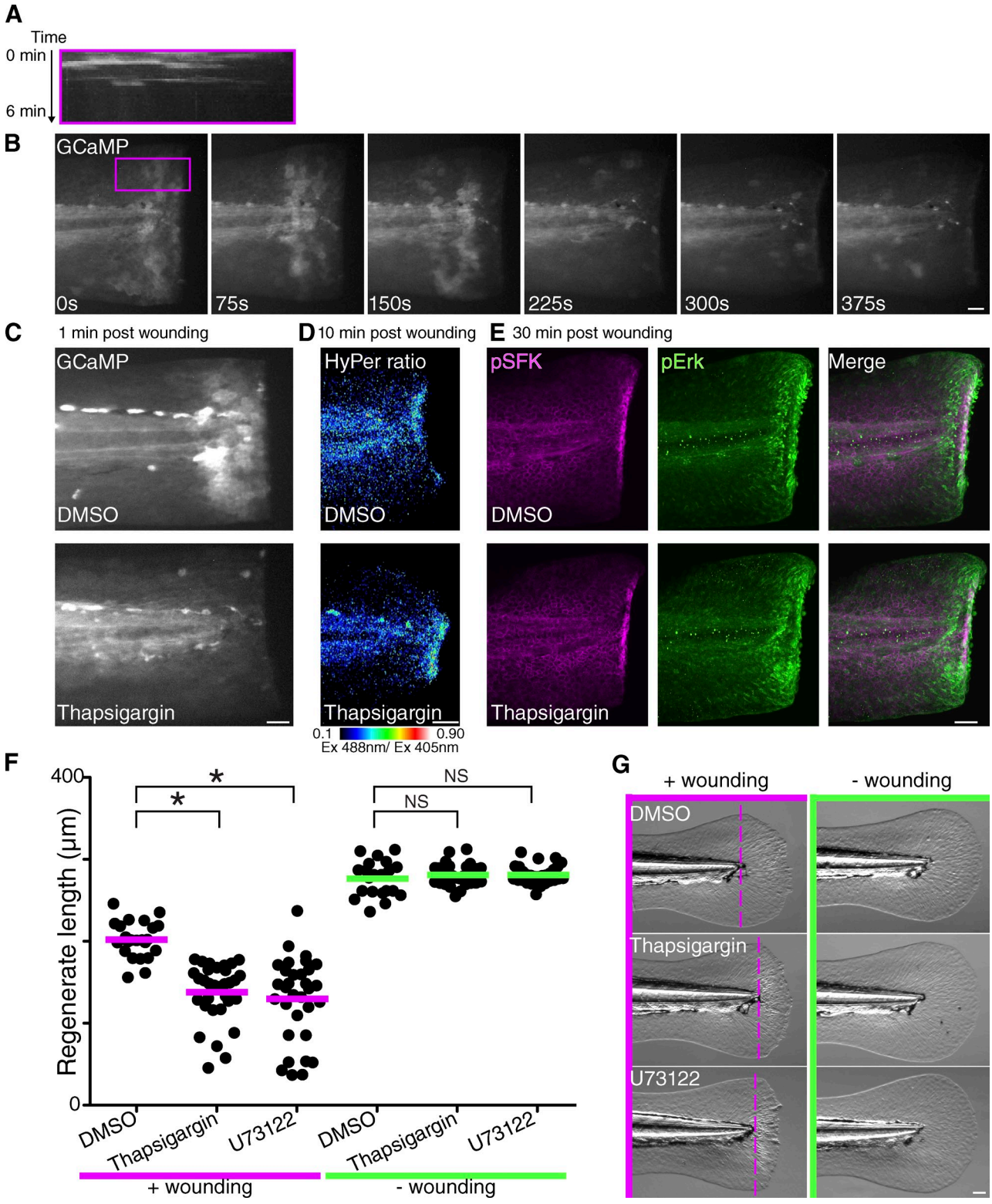

Figure 3. **Wound-induced Ca^{2+} signaling is important for late regeneration.** (A) Kymograph in the rectangular box in B. The rectangular box was summed into a 1D line, and the kymograph was made. (B) Time-lapse imaging of GCaMP3 in a 2-dpf larva immediately after wounding (see Video 1). (C) GCaMP3 images in DMSO- or thapsigargin-treated 2-dpf larvae (Video 2). (D) H_2O_2 imaging with HyPer in DMSO- or thapsigargin-treated 2-dpf larvae. Thapsigargin does not inhibit H_2O_2 burst at wounds. (E) Immunofluorescence of pSFK and pErk in DMSO- or thapsigargin-treated 2-dpf larvae. Thapsigargin did not inhibit pSFK or pErk at wounds. (F) Quantification of tail fin length at 3 d after treatment (+wound/DMSO: 23 larvae; +wound/thapsigargin: 32 larvae; +wound/U73122: 32 larvae; −wound/DMSO: 21 larvae; −wound/thapsigargin: 32 larvae; −wound/U73122: 30 larvae). Horizontal lines indicate means. (G) Representative pictures at 3 d after treatment. 2-dpf larvae were treated and wounded as described in Fig. 2 A. Dotted lines indicate tail transection. *, $P < 0.05$; one-way ANOVA with Dunnett's posttest. Ex, excitation. Bars, 50 µm.

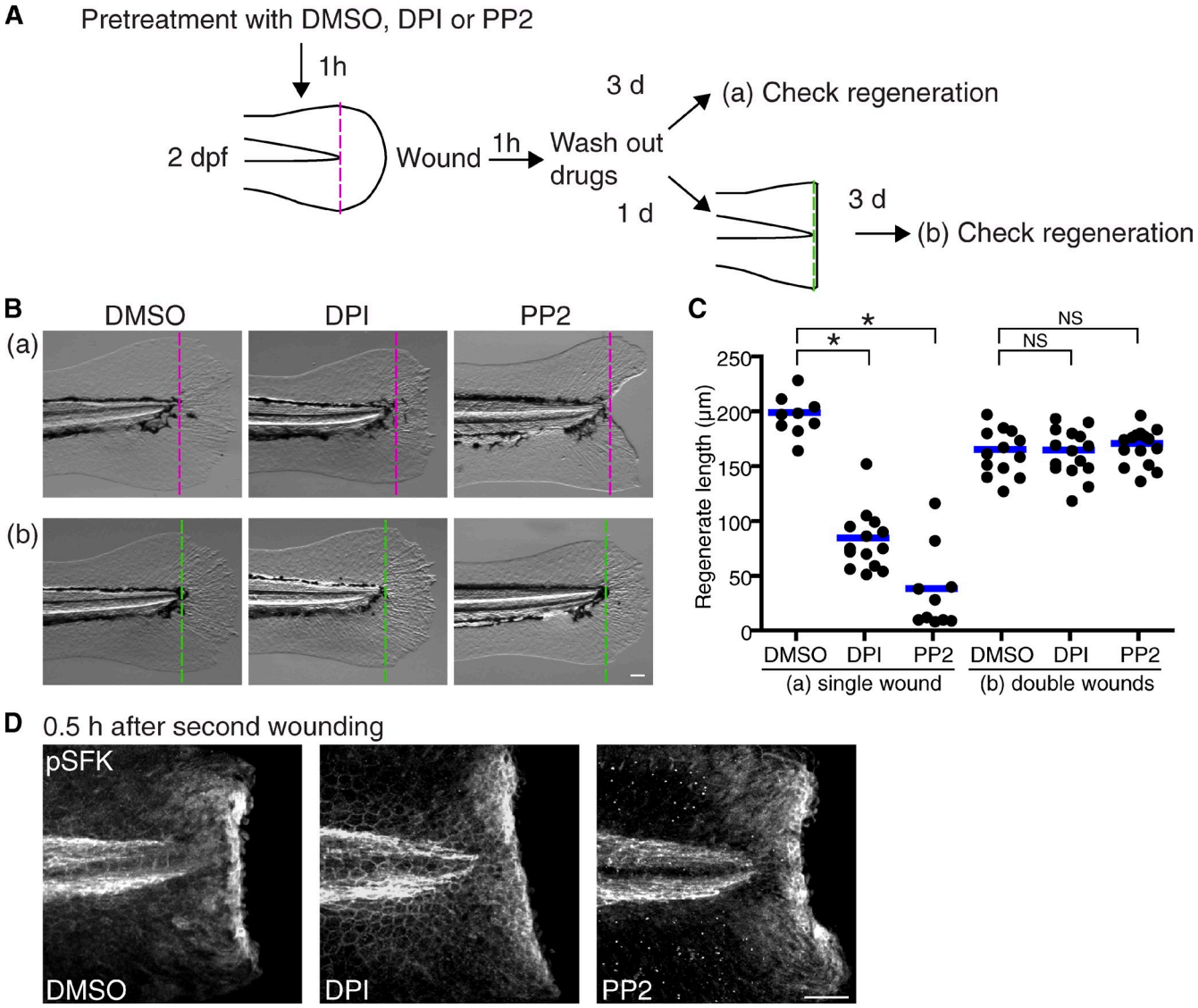

Figure 4. **Second injury induces regeneration in regeneration-defective wounds.** (A) Diagram of the double-wounding assay. (B) Representative pictures of single-wounded larvae (a) and double-wounded larvae (b) at 3 d after wounding. Dotted lines indicate tail transection. (C) Quantification of regenerated tail fin length at 3 d after wounding (single wound/DMSO: 9 larvae; single wound/DPI: 14 larvae; single wound/PP2: 10 larvae; double wound/DMSO: 13 larvae; double wound/DPI: 15 larvae; double wound/PP2: 15 larvae). Horizontal lines indicate means. (D) Immunofluorescence of pSFK at 0.5 h after second wounding. *, $P < 0.05$; one-way ANOVA with Dunnett's posttest. Bars, 50 µm.

for regeneration, we performed MO-mediated knockdown of Yes and/or Fynb. We designed MOs to target pre-mRNA splice sites. Two MOs for *fynb* and one MO for *yes* readily inhibited splicing of the respective mRNA transcripts at 2–3 dpf (Fig. 5 C). Although knockdown of Fynb and/or Yes altered the tail fin width in unwounded larvae, knockdown did not have any effect on fin length in unwounded larvae (Fig. S3, C–E). In general, fin length is what has been quantified in regeneration studies (Mathew et al., 2007; Ishida et al., 2010; Nachtrab et al., 2011). Thus, throughout this study, we focused on fin length, which was not affected by any MO treatments without wounding. We found that Fynb, but not Yes, knockdown impaired regeneration at 3 d after wounding (Fig. 5, D and E). FYN knockout mice show defects in keratinocyte differentiation in addition to other phenotypes (Calautti et al., 1995; Cabodi et al., 2000; Saito et al., 2010), whereas YES knockout mice do not show an overt phenotype (Stein et al., 1994). Moreover, FYN, but not YES, mediates redox signaling (Abe and Berk, 1999; Hehner et al., 2000; Sanguinetti et al., 2003; Li et al., 2007). Double knockdown of Fynb and Yes was challenging because of developmental defects consistent with a previous study (Jopling and den Hertog, 2005), but there was no significant difference in the fin regeneration length between single knockdown of Fynb and double knockdown of Fynb and Yes. These findings suggest that Fynb, but not Yes, is necessary for fin regeneration. In situ hybridization detected *fynb* mRNA in the tail fin (Fig. 5 F). Moreover, Fynb knockdown decreased injury-induced SFK activation at wounds and blastemal cell proliferation in regenerating fins (Fig. 5, G–I), further supporting the idea that Fynb is the SFK that regulates wound responses and regeneration.

Here, we found that early redox and SFK signaling regulates late epimorphic regeneration in zebrafish larvae. How initial

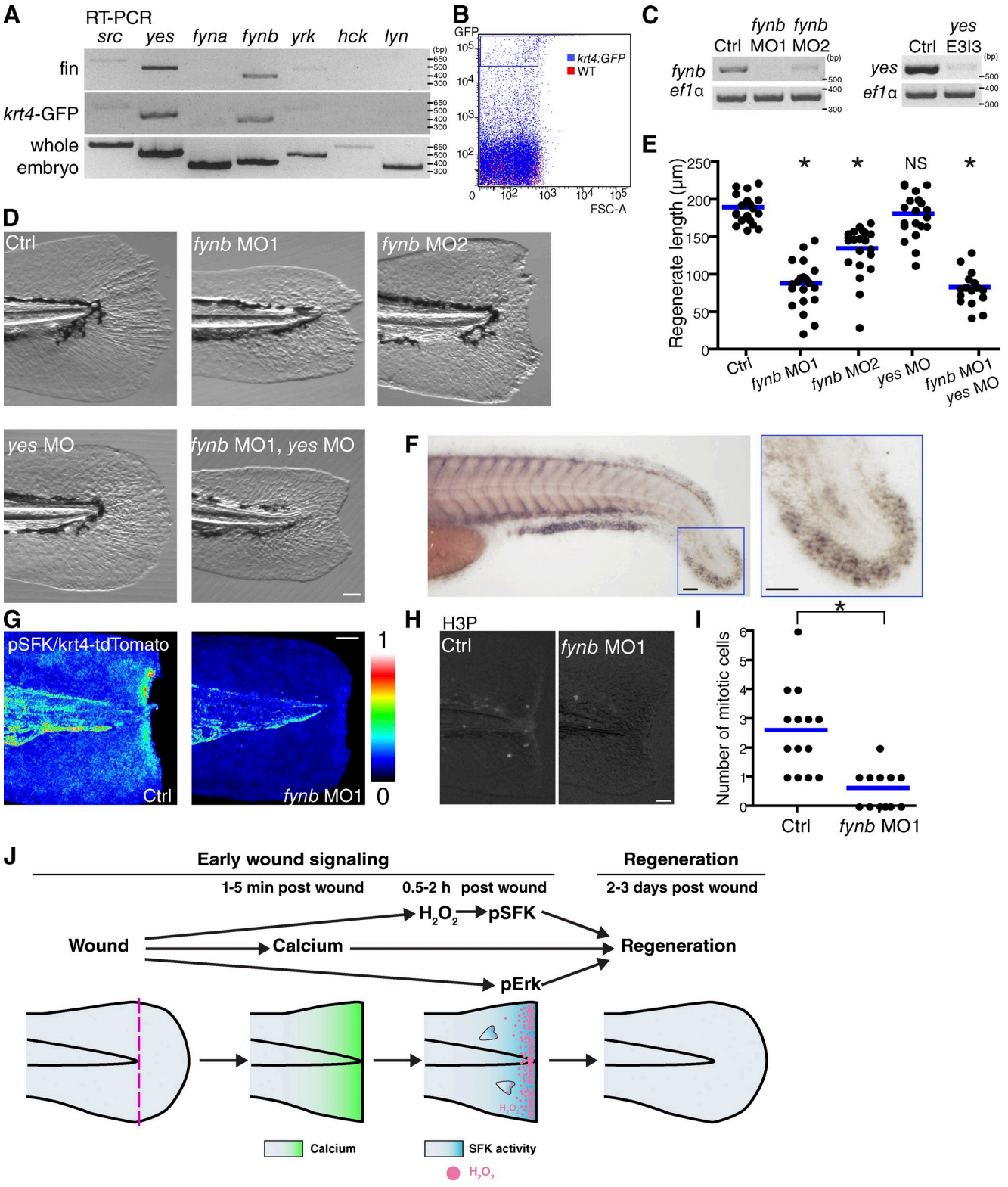

Figure 5. **Fynb is responsible for epimorphic regeneration.** (A) RT-PCR of SFKs. *hck* and *lyn*, hematopoietic-specific SFKs, are negative controls. (B) *Tg(krt4:GFP)* larvae at 3 dpf were used for flow cytometry. GFP high fractions (boxed with a blue line) were sorted. Cells from wild-type larvae were used to set the background level of autofluorescence. (C) RT-PCR of fynb and yes with/without MOs. *ef1-α* is the loading control. (D) Representative pictures at 3 d after wounding. (E) Quantification of regenerated tail fin length at 3 d after wounding (control [Ctrl]: 19 larvae; *fynb* MO1: 20 larvae; *fynb* MO2: 21 larvae; *yes* MO: 20 larvae; *fynb* MO1/*yes* MO: 16 larvae). (F) In situ hybridization of *fynb* mRNA in 2-dpf larvae. The tail fin in the blue box is magnified on the right. (G) Ratio images of pSFK/krt4-tdTomato in control and fynb morphants. (H) Mitotic cells were detected by antibody staining for phosphorylated histone H3 (H3P) at 36 h after wounding. (I) Quantification of blastemal proliferation at 36 h after wounding (control: 14 larvae; *fynb* MO1: 12 larvae). (J) A proposed model showing early wound signaling-mediated regulation of late regeneration. (E and I) *, $P < 0.05$; one-way ANOVA with Dunnett's posttest (E) and two-tailed unpaired *t* test (I). Horizontal lines indicate means. Bars, 50 μm.

wound signals boost late regeneration has not been fully explored. We have shown that redox and SFK signaling mainly function at the very early phase within 1 h after wounding. This early wound signaling "jump starts" regeneration. This concept was further supported by impaired regeneration with inhibition of other early wound signals, including Ca^{2+} and Erk signaling, which seem to work independently of redox-SFK signaling. These phenotypes are similar to the effects of glucocorticoids, which inhibit regeneration only when they are administered within a few hours after wounding (Mathew et al., 2007). Thus, redox and SFK, Ca^{2+}, and/or Erk signaling may share some downstream components with glucocorticoid-mediated signaling.

Our findings are consistent with a recent study that Duox knockdown inhibits fin regeneration in zebrafish larvae (Rieger and Sagasti, 2011). H_2O_2 is generated at wounds and promotes wound healing in mice (Roy et al., 2006). Redox and SFK signaling also regulate wound responses in *Drosophila* embryos (Juarez et al., 2011), suggesting that the redox and SFK signaling might be a phylogenetically conserved wound response.

We also found that an SFK, Fynb, is important for fin regeneration. Epithelial cells in tail fins express mRNA of *yes*, but Yes is not important for fin regeneration. It will be interesting to elucidate what functions Yes and other SFKs demonstrate in zebrafish. Although we did not rule out the possibility that Fynb might mediate regeneration functions in cells other than epithelial cells, the combination of SFK activation at wounded epithelia dependent on Fynb and functional analysis with *fynb* MOs suggests that Fynb is likely to work at injured epithelia during regeneration. How the early H_2O_2-SFK signaling regulates late regeneration remains elusive. Appendage regeneration in teleosts and amphibians is generally mediated by blastemal proliferation of fate-restricted progenitor cells (Kragl et al., 2009; Poss, 2010; Knopf et al., 2011; Tanaka and Reddien, 2011; Yoshinari and Kawakami, 2011). Our data show that inhibition of redox and SFK signaling impairs blastemal proliferation. Considering the known role of FYN in regulating keratinocyte differentiation in mammals (Calautti et al., 1995; Cabodi et al., 2000; Saito et al., 2010), it is also possible that Fynb regulates differentiation of epithelial cells in addition to blastemal proliferation. What molecular mechanisms mediate the memory effect remains to be determined, but transcription factors, such as Jun (Ishida et al., 2010), or epigenetic modifications, such as histone demethylation (Stewart et al., 2009), are likely to function downstream of redox and SFK signaling.

Together with our previous findings that leukocytes use Lyn as a redox sensor to detect H_2O_2 at wounds, our current findings suggest that redox-SFK signaling is an early wound signal that integrates wound responses in immune cells and epithelial cells (Fig. 5 J). Regeneration is a challenge in modern medicine. We speculate that it might be possible to induce regeneration in injured human tissues by providing optimal stimulation if we understand the detailed molecular mechanisms of wound healing and regeneration in regenerative organisms.

Materials and methods

Zebrafish maintenance and general procedures

Adult AB zebrafish and larvae were maintained as described previously (Yoo et al., 2010). For wounding assays, 2–3-dpf larvae were anesthetized in E3 containing 0.2 mg/ml Tricaine (ethyl 3-aminobenzoate; Sigma-Aldrich). To prevent pigment formation, some larvae were maintained in E3 containing 0.2 mM *N*-phenylthiourea (Sigma-Aldrich). Afterwards, drugs were used with 1% DMSO (20 µM PP2, 20 µM PP3, 100 µM DPI, 1 µM thapsigargin, 1 µM U73122, and 100 µM PD98059).

Regeneration assays

For regeneration assays, tail transection was performed on 2–2.5-dpf larvae using a razor blade. Regenerate length was quantified by measuring the distance between the caudal tip of the notochord and the caudal tip of the tail fin at 3 d after wounding.

Immunofluorescence and Sudan black staining

2.5–3-dpf larvae were fixed with 1.5% formaldehyde in 0.1 M Pipes, 1.0 mM $MgSO_4$, and 2 mM EGTA overnight at 4°C and immunolabeled as previously described (Yoo et al., 2011). We used the following primary antibodies: rabbit antiphospho-Src family (Tyr416) antibody (#2101; Cell Signaling Technology) at 1:300, rabbit antiphospho-Src family (Tyr416) antibody (D49G4; Cell Signaling Technology) at 1:300, mouse antiphospho-Erk1/2 (T185, Y187, T202, and Y204) antibody (ab50011; Abcam) at 1:300, mouse antipan-Cadherin antibody (CH-19 and ab6528; Abcam) at 1:300, and rabbit antiphospho–histone H3 (Ser10; #06-570; EMD Millipore) at 1:300. DyLight 488– or 549–conjugated IgG antibodies (Jackson ImmunoResearch Laboratories, Inc.) were used as secondary antibodies. Confocal immunofluorescence images were acquired with a confocal microscope (FluoView FV1000; Olympus) using a NA 0.75/20× objective. Each fluorescence channel and the differential interference contrast images were acquired by sequential line scanning. Z series were acquired using 260–600-µm pinhole and 2–10-µm step sizes. Z series images were stacked or 3D reconstructed by the FluoView FV1000 software. For Sudan black staining, embryos were fixed 1 h after wounding in 4% formaldehyde in PBS for 1.5 h at room temperature, rinsed in PBS, and incubated in 0.03% Sudan black followed by extensive washing in 70% ethanol. After rehydration to PBST (0.1% Tween 20), pigments were removed by incubation in 1% H_2O_2 and 1% KOH solution. Embryos were observed using a zoom microscope (SMZ1500; Nikon).

FACS and RT-PCR

Trypsin-dissociated cells of *Tg(krt4:GFP)* (a gift from G.A. Smolen, Agios Pharmaceuticals, Cambridge, MA) at 3 dpf were sorted by FACS using dissociated cells of wild-type larvae as the background level of autofluorescence (Yoo and Huttenlocher, 2011). RNA was isolated using the RNeasy Mini kit (QIAGEN), and one-step RT-PCR (QIAGEN) was performed. Primers for *src*, *yrk*, *hck*, and *lyn* have been previously described (Yoo et al., 2011). Other oligonucleotide sequences were as follows: *fyna* forward, 5′-CTTCCATGCGCCTGTCAGTC-3′; *fyna* reverse, 5′-GATTTCCATTTGACAGCAGTTGTCG-3′; *fynb* forward, 5′-CAGCGGGACCGGAACTGCTG-3′; *fynb* reverse, 5′-CCCTGTAGAAAGAAGCTGCCTC-3′; *yes* forward, 5′-GGCCTCTATGGACCAGACCC-3′; and *yes* reverse, 5′-CTTTAGTGGTCTCACTTTCTCGGAC-3′.

MO injection and RT-PCR

MO oligonucleotides (Gene Tools) in Danieau buffer (58 mM NaCl, 0.7 mM KCl, 0.4 mM $MgSO_4$, 0.6 mM $Ca(NO_3)_2$, and 5.0 mM Hepes, pH 7.1–7.3) were injected (3 nL) into one-cell-stage embryos. For Pu.1 knockdown, *pu.1* MO (5′-GATATACTGATACTCCATTGGTGGT-3′; Rhodes et al., 2005) was used at 500 µM. For Duox knockdown, *duox* MO (5′-AGTGAATTAGAGAAATGCACCTTTT-3′) was used (Yoo et al., 2011). For Fynb knockdown, 150 µM *fynb* splice MO *fynb* MO1 (5′-GGAGTAAGTAGAGGACATCACCTTT-3′) or 150 µM *fynb* splice MO *fynb* MO2 (5′-GATCTTAATACTTACGTGCTGTTGA-3′) was used. For Yes knockdown, 500 µM *yes* splice MO (5′-CTCTTAATCGAAGGACTCACGTGTT-3′) was used. Danieau buffer was used as a control. For morphotyping of the splicing MOs, RNA was prepared from 2.5–3-dpf larvae using TRIZOL (Invitrogen), and one-step RT-PCR was performed. Oligonucleotide sequences used for RT-PCR were as follows: *fynb* forward, 5′-CAGCGGGACCGGAACTGCTG-3′; *fynb* reverse, 5′-GGTCTCGAACTGAGCTCTAGTGG-3′; *yes* forward, 5′-GGCCTCTATGGACCAGACCC-3′; and *yes* reverse, 5′-CGTTGTCTCCCTTCATCTCATCCC-3′.

Whole-mount in situ hybridization

For in situ hybridization, 1.8 kb of zebrafish *fynb* was amplified with the T7 promoter by PCR using clone 7275006 (Thermo Fisher Scientific) as a template. A digoxigenin-labeled RNA probe was transcribed with the use of T7 RNA polymerase (Ambion). 2-dpf larvae were fixed in 4% paraformaldehyde in PBS, and mRNA was labeled by in situ hybridization as previously described (Yoo et al., 2011). Oligonucleotide sequences used for PCR were as follows: *fynb* forward, 5′-GCGAGAAGAAGCTCTTTGGA-3′, and *fynb* T7 reverse, 5′-TAATACGACTCACTATAGGGACCCACAATTCCTGCTGTTC-3′.

Live imaging and ratiometric analysis

GCaMP3 (Tian et al., 2009) was subcloned into the pCS2+ vector, linearized by Not1, and in vitro transcribed by SP6 RNA polymerase (Invitrogen). Approximately 5 nl of a solution containing 75 ng/µl GCaMP3 mRNA was injected into one-cell-stage embryos, and live imaging was performed with a stereomicroscope (SMZ1500) at 2 dpf. H_2O_2 imaging was performed as previously described (Yoo et al., 2011). In brief, HyPer fluorescence was excited with 405- and 488-nm lasers, and emission wavelengths of 505–510 and 510–525 nm (dichroic mirror: SDM510; band pass filter: BA505-525; Olympus) were acquired using the sequential line scanning. Ratiometric analysis was performed by using FluoView FV1000 software. 2D ratiometric images were made after z series stacking, or 3D reconstruction was performed by making ratiometric images for each z series. Two different methods were used to create ratiometric images to exclude possible artifacts produced in the process of making ratiometric pictures. In the first method, after complete loss of background by subtraction in the numerator channel, ratio images were made by dividing the numerator channel with the denominator channel and processed by a median filter to remove background noise. In the second method, after subtraction of background both in numerator and denominator channels, ratio images were made by dividing the numerator channel with the denominator channel. After that, binary images made by thresholding the numerator channel were combined with the ratio images using a logical AND and processed by a median filter.

Statistics

Assuming a Gaussian distribution of the overall population of values, p-values were driven by two-tailed paired *t* test or one-way analysis of variance (ANOVA) with Dunnett's posttest. Data are representative of at least three separate experiments.

Online supplemental material

Fig. S1 shows data of redox and SFK signaling at wounds. Fig. S2 shows that early redox and SFK signaling regulates late resolution of inflammation. Fig. S3 shows data of early wound signaling components. Video 1 shows live imaging of a GCaMP3 probe immediately after wounding. Video 2 shows live imaging of a GCaMP3 probe in DMSO- or thapsigargin-treated larvae. Online supplemental material is available at http://www.jcb.org/cgi/content/full/jcb.201203154/DC1.

We thank G.A. Smolen for the generous gift of *Tg(krt4:GFP)* and T.W. Starnes for insightful discussion and critical reading of the manuscript.

This work was supported by American Heart Association fellowship grant 11PRE4890041 (to S.K. Yoo), National Institute of Environmental Health Sciences grant ES007015 (to C.M. Freisinger), National Cancer Institute grant CA157322 (to C.M. Freisinger), and National Institutes of Health grant GM074827 (to A. Huttenlocher).

Submitted: 29 March 2012
Accepted: 10 September 2012

References

Abe, J., and B.C. Berk. 1999. Fyn and JAK2 mediate Ras activation by reactive oxygen species. *J. Biol. Chem.* 274:21003–21010. http://dx.doi.org/10.1074/jbc.274.30.21003

Bienert, G.P., J.K. Schjoerring, and T.P. Jahn. 2006. Membrane transport of hydrogen peroxide. *Biochim. Biophys. Acta*. 1758:994–1003. http://dx.doi.org/10.1016/j.bbamem.2006.02.015

Cabodi, S., E. Calautti, C. Talora, T. Kuroki, P.L. Stein, and G.P. Dotto. 2000. A PKC-eta/Fyn-dependent pathway leading to keratinocyte growth arrest and differentiation. *Mol. Cell*. 6:1121–1129. http://dx.doi.org/10.1016/S1097-2765(00)00110-6

Calautti, E., C. Missero, P.L. Stein, R.M. Ezzell, and G.P. Dotto. 1995. fyn tyrosine kinase is involved in keratinocyte differentiation control. *Genes Dev.* 9:2279–2291. http://dx.doi.org/10.1101/gad.9.18.2279

Feng, Y., C. Santoriello, M. Mione, A. Hurlstone, and P. Martin. 2010. Live imaging of innate immune cell sensing of transformed cells in zebrafish larvae: parallels between tumor initiation and wound inflammation. *PLoS Biol.* 8:e1000562. http://dx.doi.org/10.1371/journal.pbio.1000562

Giannoni, E., F. Buricchi, G. Raugei, G. Ramponi, and P. Chiarugi. 2005. Intracellular reactive oxygen species activate Src tyrosine kinase during cell adhesion and anchorage-dependent cell growth. *Mol. Cell. Biol.* 25:6391–6403. http://dx.doi.org/10.1128/MCB.25.15.6391-6403.2005

Gong, Z., B. Ju, X. Wang, J. He, H. Wan, P.M. Sudha, and T. Yan. 2002. Green fluorescent protein expression in germ-line transmitted transgenic zebrafish under a stratified epithelial promoter from keratin8. *Dev. Dyn.* 223:204–215. http://dx.doi.org/10.1002/dvdy.10051

Hehner, S.P., R. Breitkreutz, G. Shubinsky, H. Unsoeld, K. Schulze-Osthoff, M.L. Schmitz, and W. Dröge. 2000. Enhancement of T cell receptor signaling by a mild oxidative shift in the intracellular thiol pool. *J. Immunol.* 165:4319–4328.

Ishida, T., T. Nakajima, A. Kudo, and A. Kawakami. 2010. Phosphorylation of Junb family proteins by the Jun N-terminal kinase supports tissue regeneration in zebrafish. *Dev. Biol.* 340:468–479. http://dx.doi.org/10.1016/j.ydbio.2010.01.036

Jopling, C., and J. den Hertog. 2005. Fyn/Yes and non-canonical Wnt signalling converge on RhoA in vertebrate gastrulation cell movements. *EMBO Rep.* 6:426–431. http://dx.doi.org/10.1038/sj.embor.7400386

Juarez, M.T., R.A. Patterson, E. Sandoval-Guillen, and W. McGinnis. 2011. Duox, Flotillin-2, and Src42A are required to activate or delimit the spread of the transcriptional response to epidermal wounds in *Drosophila*. *PLoS Genet.* 7:e1002424. http://dx.doi.org/10.1371/journal.pgen.1002424

Kemble, D.J., and G. Sun. 2009. Direct and specific inactivation of protein tyrosine kinases in the Src and FGFR families by reversible cysteine oxidation. *Proc. Natl. Acad. Sci. USA*. 106:5070–5075. http://dx.doi.org/10.1073/pnas.0806117106

Knopf, F., C. Hammond, A. Chekuru, T. Kurth, S. Hans, C.W. Weber, G. Mahatma, S. Fisher, M. Brand, S. Schulte-Merker, and G. Weidinger. 2011. Bone regenerates via dedifferentiation of osteoblasts in the zebrafish fin. *Dev. Cell*. 20:713–724. http://dx.doi.org/10.1016/j.devcel.2011.04.014

Kragl, M., D. Knapp, E. Nacu, S. Khattak, M. Maden, H.H. Epperlein, and E.M. Tanaka. 2009. Cells keep a memory of their tissue origin during axolotl limb regeneration. *Nature*. 460:60–65. http://dx.doi.org/10.1038/nature08152

Le Guyader, D., M.J. Redd, E. Colucci-Guyon, E. Murayama, K. Kissa, V. Briolat, E. Mordelet, A. Zapata, H. Shinomiya, and P. Herbomel. 2008. Origins and unconventional behavior of neutrophils in developing zebrafish. *Blood*. 111:132–141. http://dx.doi.org/10.1182/blood-2007-06-095398

Li, Z., T. Dong, C. Pröschel, and M. Noble. 2007. Chemically diverse toxicants converge on Fyn and c-Cbl to disrupt precursor cell function. *PLoS Biol.* 5:e35. http://dx.doi.org/10.1371/journal.pbio.0050035

Martin, G.S. 2001. The hunting of the Src. *Nat. Rev. Mol. Cell Biol.* 2:467–475. http://dx.doi.org/10.1038/35073094

Martin, P. 1997. Wound healing—aiming for perfect skin regeneration. *Science*. 276:75–81. http://dx.doi.org/10.1126/science.276.5309.75

Martin, P., and S.J. Leibovich. 2005. Inflammatory cells during wound repair: the good, the bad and the ugly. *Trends Cell Biol.* 15:599–607. http://dx.doi.org/10.1016/j.tcb.2005.09.002

Mathew, L.K., S. Sengupta, A. Kawakami, E.A. Andreasen, C.V. Löhr, C.A. Loynes, S.A. Renshaw, R.T. Peterson, and R.L. Tanguay. 2007. Unraveling tissue regeneration pathways using chemical genetics. *J. Biol. Chem.* 282:35202–35210. http://dx.doi.org/10.1074/jbc.M706640200

Mathias, J.R., B.J. Perrin, T.X. Liu, J. Kanki, A.T. Look, and A. Huttenlocher. 2006. Resolution of inflammation by retrograde chemotaxis of neutrophils in transgenic zebrafish. *J. Leukoc. Biol.* 80:1281–1288. http://dx.doi.org/10.1189/jlb.0506346

Moreira, S., B. Stramer, I. Evans, W. Wood, and P. Martin. 2010. Prioritization of competing damage and developmental signals by migrating macrophages in the *Drosophila* embryo. *Curr. Biol.* 20:464–470. http://dx.doi.org/10.1016/j.cub.2010.01.047

Nachtrab, G., M. Czerwinski, and K.D. Poss. 2011. Sexually dimorphic fin regeneration in zebrafish controlled by androgen/GSK3 signaling. *Curr. Biol.* 21:1912–1917. http://dx.doi.org/10.1016/j.cub.2011.09.050

Niethammer, P., C. Grabher, A.T. Look, and T.J. Mitchison. 2009. A tissue-scale gradient of hydrogen peroxide mediates rapid wound detection in zebrafish. *Nature*. 459:996–999. http://dx.doi.org/10.1038/nature08119

Orozco-Cárdenas, M.L., J. Narváez-Vásquez, and C.A. Ryan. 2001. Hydrogen peroxide acts as a second messenger for the induction of defense genes in

tomato plants in response to wounding, systemin, and methyl jasmonate . *Plant Cell*. 13:179–191.

Paulsen, C.E., and K.S. Carroll. 2010. Orchestrating redox signaling networks through regulatory cysteine switches. *ACS Chem. Biol.* 5:47–62. http://dx.doi.org/10.1021/cb900258z

Poole, L.B., and K.J. Nelson. 2008. Discovering mechanisms of signaling-mediated cysteine oxidation. *Curr. Opin. Chem. Biol.* 12:18–24. http://dx.doi.org/10.1016/j.cbpa.2008.01.021

Poss, K.D. 2010. Advances in understanding tissue regenerative capacity and mechanisms in animals. *Nat. Rev. Genet*. 11:710–722. http://dx.doi.org/10.1038/nrg2879

Rhee, S.G. 2006. Cell signaling. H2O2, a necessary evil for cell signaling. *Science*. 312:1882–1883. http://dx.doi.org/10.1126/science.1130481

Rhodes, J., A. Hagen, K. Hsu, M. Deng, T.X. Liu, A.T. Look, and J.P. Kanki. 2005. Interplay of pu.1 and gata1 determines myelo-erythroid progenitor cell fate in zebrafish. *Dev. Cell*. 8:97–108. http://dx.doi.org/10.1016/j.devcel.2004.11.014

Rieger, S., and A. Sagasti. 2011. Hydrogen peroxide promotes injury-induced peripheral sensory axon regeneration in the zebrafish skin. *PLoS Biol.* 9:e1000621. http://dx.doi.org/10.1371/journal.pbio.1000621

Roy, S., S. Khanna, K. Nallu, T.K. Hunt, and C.K. Sen. 2006. Dermal wound healing is subject to redox control. *Mol. Ther.* 13:211–220. http://dx.doi.org/10.1016/j.ymthe.2005.07.684

Saito, Y.D., A.R. Jensen, R. Salgia, and E.M. Posadas. 2010. Fyn: a novel molecular target in cancer. *Cancer*. 116:1629–1637. http://dx.doi.org/10.1002/cncr.24879

Sanguinetti, A.R., H. Cao, and C. Corley Mastick. 2003. Fyn is required for oxidative- and hyperosmotic-stress-induced tyrosine phosphorylation of caveolin-1. *Biochem. J.* 376:159–168. http://dx.doi.org/10.1042/BJ20030336

Sicheri, F., I. Moarefi, and J. Kuriyan. 1997. Crystal structure of the Src family tyrosine kinase Hck. *Nature*. 385:602–609. http://dx.doi.org/10.1038/385602a0

Stein, P.L., H. Vogel, and P. Soriano. 1994. Combined deficiencies of Src, Fyn, and Yes tyrosine kinases in mutant mice. *Genes Dev.* 8:1999–2007. http://dx.doi.org/10.1101/gad.8.17.1999

Stewart, S., Z.Y. Tsun, and J.C. Izpisua Belmonte. 2009. A histone demethylase is necessary for regeneration in zebrafish. *Proc. Natl. Acad. Sci. USA*. 106:19889–19894.

Tanaka, E.M., and P.W. Reddien. 2011. The cellular basis for animal regeneration. *Dev. Cell*. 21:172–185. http://dx.doi.org/10.1016/j.devcel.2011.06.016

Tian, L., S.A. Hires, T. Mao, D. Huber, M.E. Chiappe, S.H. Chalasani, L. Petreanu, J. Akerboom, S.A. McKinney, E.R. Schreiter, et al. 2009. Imaging neural activity in worms, flies and mice with improved GCaMP calcium indicators. *Nat. Methods*. 6:875–881. http://dx.doi.org/10.1038/nmeth.1398

Wood, W. 2012. Wound healing: calcium flashes illuminate early events. *Curr. Biol.* 22:R14–R16. http://dx.doi.org/10.1016/j.cub.2011.11.019

Xu, S., and A.D. Chisholm. 2011. A Gαq-Ca^{2+} signaling pathway promotes actin-mediated epidermal wound closure in *C. elegans. Curr. Biol.* 21:1960–1967. http://dx.doi.org/10.1016/j.cub.2011.10.050

Xu, W., S.C. Harrison, and M.J. Eck. 1997. Three-dimensional structure of the tyrosine kinase c-Src. *Nature*. 385:595–602. http://dx.doi.org/10.1038/385595a0

Yeatman, T.J. 2004. A renaissance for SRC. *Nat. Rev. Cancer*. 4:470–480. http://dx.doi.org/10.1038/nrc1366

Yoo, S.K., and A. Huttenlocher. 2011. Spatiotemporal photolabeling of neutrophil trafficking during inflammation in live zebrafish. *J. Leukoc. Biol.* 89:661–667. http://dx.doi.org/10.1189/jlb.1010567

Yoo, S.K., Q. Deng, P.J. Cavnar, Y.I. Wu, K.M. Hahn, and A. Huttenlocher. 2010. Differential regulation of protrusion and polarity by PI3K during neutrophil motility in live zebrafish. *Dev. Cell*. 18:226–236. http://dx.doi.org/10.1016/j.devcel.2009.11.015

Yoo, S.K., T.W. Starnes, Q. Deng, and A. Huttenlocher. 2011. Lyn is a redox sensor that mediates leukocyte wound attraction in vivo. *Nature*. 480:109–112. http://dx.doi.org/10.1038/nature10632

Yoshinari, N., and A. Kawakami. 2011. Mature and juvenile tissue models of regeneration in small fish species. *Biol. Bull.* 221:62–78.